4B.8 THE RAPID INTENSIFICATION OF HURRICANE GUILLERMO (1997) AS VIEWED WITH GPS DROPWINDSONDES

Matthew Sitkowski, Klaus Dolling, Gary Barnes
Department of Meteorology, University of Hawaii, Honolulu, Hawaii

1. INTRODUCTION

On August 2nd and 3rd of 1997 the two NOAA WP-3D aircraft simultaneously sampled Hurricane Guillermo in the eastern Pacific as part of the Vortex Motion and Evolution Experiment. This was the first experiment to deploy Global Positioning System dropwindsondes (GPS sondes) into a hurricane. Over 80 GPS sondes were jettisoned from 500 and 700 hPa within 300 km of the hurricane center over the two days. On each day, the lower aircraft visited the center 10 times as the hurricane progressed steadily westward near 5 m s^{-1}. This pattern allows for frequent monitoring of the reflectivity fields of the eyewall with the lower fuselage and tail radars. Sampling of the storm occurred just as rapid intensification (RI) commenced on August 2nd with the hurricane deepening 25 hPa by the time the aircraft returned to a steady-state hurricane on August 3rd. Deepening may have been as much as 2 hPa h^{-1} on the 2nd. The experiment provides us with a unique opportunity to observe how the inner core of a hurricane evolves during an RI period. Better understanding of how the eyewall interacts with the immediate environment during RI may aid in forecasting RI.

2. DATA

The data from the GPS sondes were processed through the Atmospheric Sounding Processing Environment (APSEN) before undergoing subjective analysis by the authors. The data were treated with a cubic spline to produce horizontal fields from 4 km altitude to near the sea surface. To do this we have combined the sondes for each day, assuming that the storm is quasi-stationary during the 6 hours of sampling. The flight paths and distribution of the GPS sondes, although denser on the 3rd, were similar enough to the 2nd so the composite fields from each day could be compared, save for the eyewall region. In-situ aircraft data with 1 Hz resolution will be used to define the sharp radial gradients associated with the eyewall. Lower fuselage and tail radar were also used for the analysis.

Corresponding author address: Matthew Sitkowski, Department of Meteorology, University of Hawaii, 2525 Correa Rd, Honolulu, HI 96822
E-mail: sitkow@hawaii.edu

3. ANALYSIS

a. Reflectivity Evolution

Lower fuselage radar reflectivity fields from the 700 hPa aircraft reveal an oval shaped eye with a crescent eyewall. On August 2nd, the eyewall repeatedly tried to close off the western side of the eye with some attempts more aggressive and successful than others. Figure 1 displays the eyewall reflectivity from 1854 UTC and 2119 UTC on August 2nd and 0003 UTC on August 3rd. Surface pressure extrapolation from the 700 hPa aircraft suggests Guillermo had its most impressive deepening near the time of the fifth pass (2119 UTC), during which the plane encountered the eyewall that entered the middle of the eye from the north. Although the band penetrated a dry, stable environment, the argument can be made that the ambient air becomes less stable as it is moistened by the band. This allowed for the following band to, at least temporarily, close off the eye. Additionally, greater reflectivity values and more banding features developed over the western portion of the storm during the sampling. The storm had a much more circular appearance on August 3rd, but still displays a wave number one reflectivity pattern with greatest values located in the eastern eyewall (Fig. 2). Comparisons between the 2 days show that the eye diameter was reduced by at least 10 km during the RI. This is consistent with RI

(a)

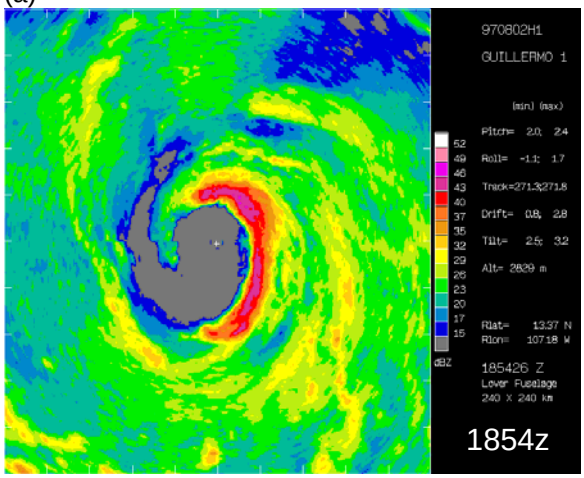

(b)

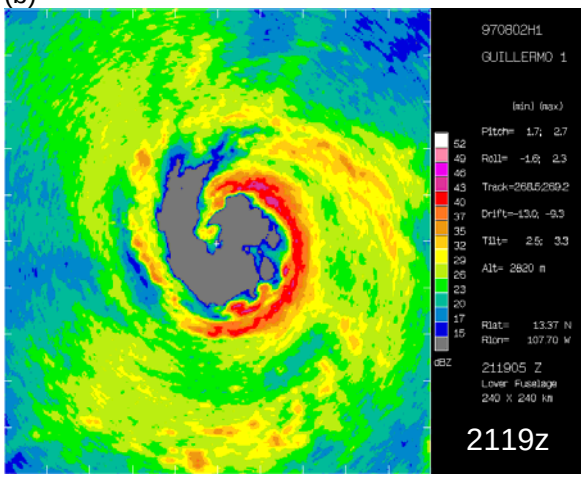

(c)

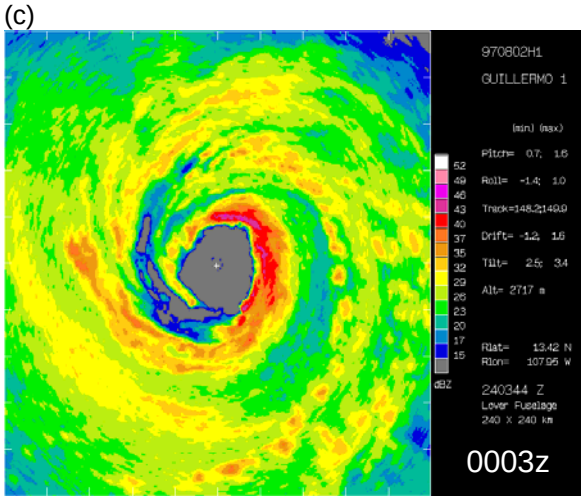

Fig. 1. 240 km x 240 km lower fuselage images taken on 02 Aug. at (a) 1854 UTC, (b) 2119 UTC, and (c) 0003 UTC 03 Aug. The aircraft was located in the eye when each image was taken.

typhoons examined by Holliday and Thompson (1979). However, echo tops, and estimated rain rate remained similar for the two days. The shrinkage of the eyewall coupled with a nearly constant rain rate implies a reduction of net latent heat release during the RI.

b. Kinematic Evolution

As expected, composite fields for tangential and radial flow contain greater values for the 3rd. However, orientation of the radial flow differed between the two days. An asymmetric pattern with maximum values observed along the east-southeast portion of the eyewall on the 2nd developed into a stronger, axisymmetric arrangement after RI concluded on Aug. 3rd (Fig. 3). Unfortunately, GPS sondes were never deployed into the eyewall on Aug. 2nd and it is not clearly known how radial flow evolved at the eyewall. However, a rather large expansion of the radial flow is exhibited on Aug. 3rd at 100 m. Inflow near 5 ms^{-1} borders the analysis at 300 km. Both days exhibit modest outflow by 2000 m altitude less than one degree latitude north of the circulation center.

c. Thermodynamic Evolution

700 hPa temperature and dewpoint readings taken in the eye on August 2nd depict greater dewpoint depressions than on the 3rd, when the storm was steady-state. Several saturated eye passes at the same level were observed on the second day and have been documented for intense hurricanes (e.g., Jordan 1952, 1961; Simpson 1952; Franklin et al. 1988). In contrast, 500 hPa dewpoint depressions were greater on Aug 03 than on Aug 02. This, along with eye temperatures above 3 km having increased as much as 5 °C between days, supports strong subsidence above 700 hPa.

Equivalent potential temperature (θ_e) near the sea surface increased 15 K during the RI. The greatest values of θ_e were located in the lowest 2 km of the eye on both days. Several other investigators (e.g., Jorgensen 1984; Schneider and Barnes 2005) have also found maximum θ_e values in the eye. Vertical profiles of θ_e in the

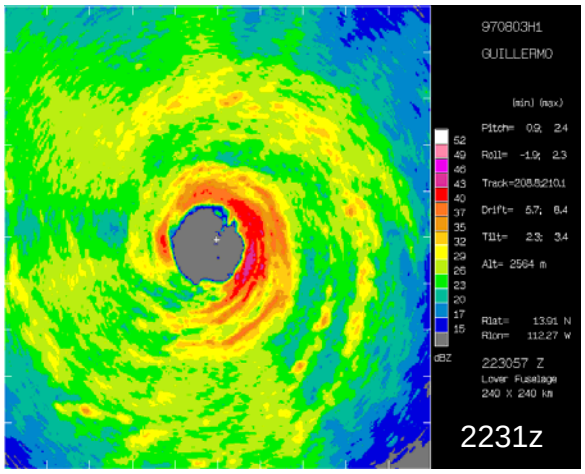

Fig. 2. 240 km x 240 km lower fuselage image taken on at 2231 UTC 03 Aug. The aircraft was located in the eye.

eyewall were homogenous from 700 hPa to the surface, whereas eye profiles of θ_e exhibit greater values from near 2 km down to the surface (Fig. 4.). The eye and eyewall profiles are intriguing and were examined by Eastin et al. (2005). They speculate that θ_e maximum in the eye was the primary source for buoyant updrafts in the eyewall and that mesovortices induced mixing in the eye allowing for θ_e in the eye to fluctuate in a short time period.

4. DISCUSSION

While this study does not attempt to determine the initial cause of RI, it does provide unprecedented low-level horizontal fields during and proceeding RI. Several thermodynamic and kinematic changes, some unexpected, were noted between the two days. The synoptic environment and storm movement changed little during RI. Table 1 is taken from Eastin et al. (2005) and lists some large scale characteristics for the two days. Synoptic conditions are currently being examined with ECMWF 2.5° resolution and should result in similar findings in Table 1. It should be noted that shear was greater during the RI and both days exceed average shear values for RI Atlantic storms calculated by Kaplan and DeMaria (2003).

Many of the structural differences, upon conclusion of RI, are confined to the lowest

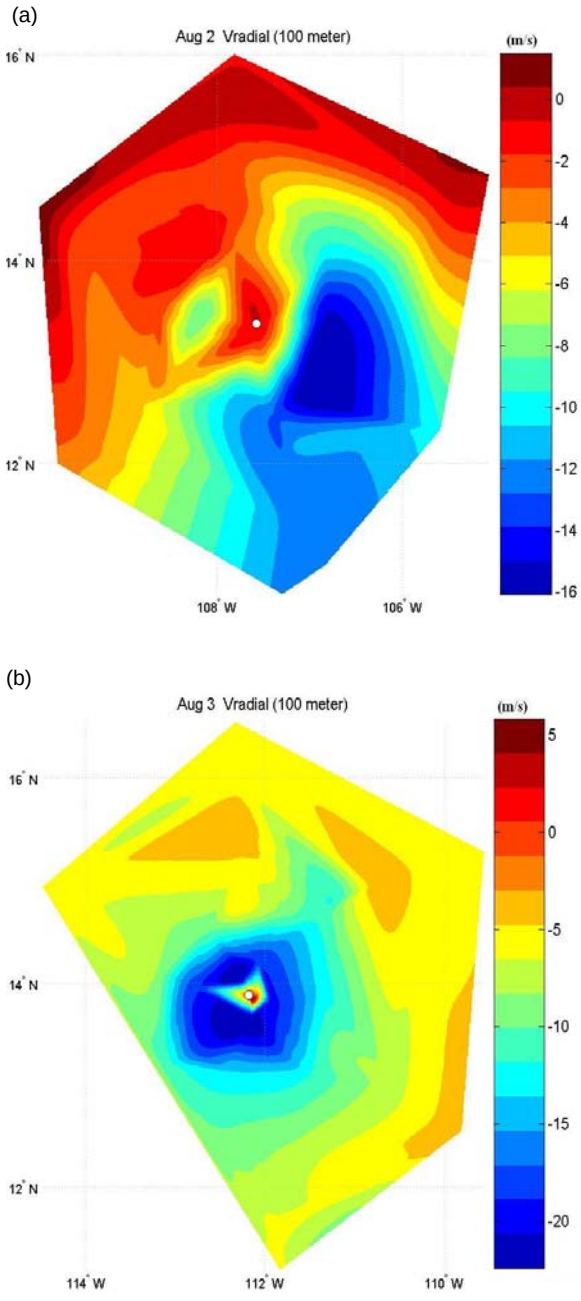

Fig. 3. Composite images of radial wind for 02 Aug. (a) and 03 Aug. (b) at 100 m. Center of the storm is represented by the white dot.

kilometer, as detected by GPS sondes. The reflectivity pattern still depicts greater values over the eastern portion of the storm and 700 hPa flight-level data contains remarkable similarities in temperature, dewpoint, wind speed, and vertical velocities. Corresponding passes through the eye maintain similar temperature profiles

Table 1. Intensity, motion, and large-scale specifics for Guillermo [From Eastin et al. 2005.]

Storm	Date yr/mo/day	Storm intensity[a] (mb)	Intensity change[a] [mb (12 h)$^{-1}$]	Storm motion[a] (m s^{-1}/degrees)	200–850-mb shear[b] (m s^{-1}/degrees)	SST[b,c] (°C)	MPI[d] (mb)
Guillermo	97/08/02	950	−28	4.5/100	8.3/355	29.9	881
	97/08/03	923	−2	5.5/95	5.9/360	29.9	881

[a] Obtained from the National Hurricane Center "best track" databases (e.g., Neumann et al. 1999).
[b] Extracted from the Statistical Hurricane Intensity Prediction Scheme (SHIPS) predictor databases (DeMaria and Kaplan 1994b, 1999).
[c] Derived from weekly SST fields (Reynolds and Smith 1993).
[d] MPI = maximum potential intensity, as defined by DeMaria and Kaplan (1994a) and using the Kraft (1961) relationship.

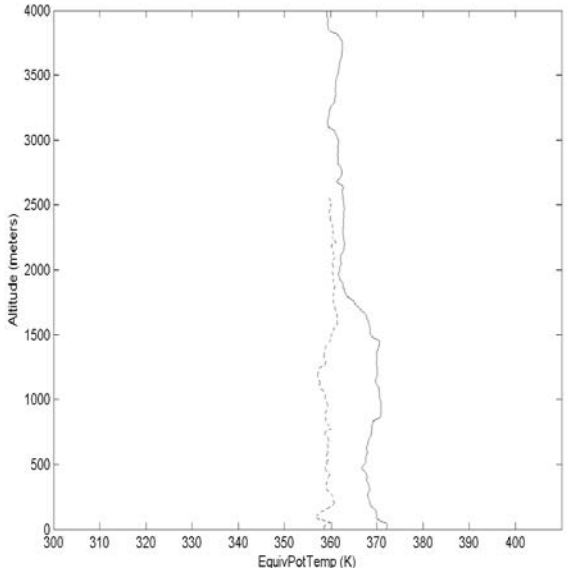

Fig. 4. Representative vertical profiles of θ_e for the eyewall (dashed) and eye (solid) on 03 Aug. Eye profiles have greater θ_e values from the surface to near 2000 m.

with matching perturbations. Although higher values were recorded on the 3rd, wind speed profiles parallel each other for several passes. Even vertical velocities tell a similar story for the two days. Areas of active updrafts and downdrafts match well on the 2nd and 3rd. This aspect of the research will continue to be investigated.

Acknowledgements. This work is supported by NSF Grant ATM-0239648. The dedication of the NOAA aircraft Operations Center and the NOAA/AOML Hurricane Research Division is greatly appreciated.

REFERENCES

Eastin, Matthew D, W. M. Gray and P. G. Black, 2005: Buoyancy of Convective Vertical Motions in the Inner Core of Intense Hurricanes. Part II: Case Studies. *Mon. Wea. Rev.*, **133**, 209–227.

Franklin, James L., S. J. Lord and F. D. Marks Jr., 1988: Dropwindsonde and Radar Observations of the Eye of Hurricane Gloria (1985). *Mon. Wea. Rev.*, **116**, 1237–1244.

Holliday, Charles R. and A. H. Thompson, 1979: Climatological Characteristics of Rapidly Intensifying Typhoons. *Mon. Wea. Rev.*, **107**, 1022–1034.

Jorgensen, David P., 1984: Mesoscale and Convective-Scale Characteristics of Mature Hurricanes. Part II. Inner Core Structure of Hurricane Allen (1980). *J. Atmos. Sci.*, **41**, 1287–1311.

Kaplan, John and M. DeMaria, 2003: Large-Scale Characteristics of Rapidly Intensifying Tropical Cyclones in the North Atlantic Basin. *Wea.Forecasting*, **18**, 1093–1108.

Schneider, Rebecca and G. M. Barnes, 2005: Low-Level Kinematic, Thermodynamic, and Reflectivity Fields Associated with Hurricane Bonnie (1998) at Landfall. *Mon. Wea. Rev.*, **133**, No. 11, 3243–3259.